Chapter 16

The Multiple Indicator Dilution Method for Input/Output Studies

Chapter Contents

16-1. Introduction

In the whole organ approach to cellular metabolism, the processes of capillary permeation, cellular entry, and intracellular reaction kinetics need to be examined in detail. The area is complex and varies from organ to organ, but there is a set of principles unifying the approaches to studies of these processes. The general approach to endogenous metabolism has been to carry out tracer studies within a variety of concentration steady states, and for xenobiotics, to study the disposition of tracer within a variety of developed and maintained steady-state bulk concentrations.

To study processes *in vivo*, a nondestructive approach is needed. The multiple-indicator dilution technique, introduced by Chinard et al. (1955), based on the use of multiple simultaneous controls, has been the approach of choice. Generally, the tracer substance under study and a reference which does not escape the capillaries are introduced simultaneously into the inflowing blood stream, and their outflow dilution curves are recorded. From a comparison of the outflow patterns for the two substances, information concerning the transcapillary passage of the study substance can be deduced. If the study substance enters tissue cells, a second reference is also usually added to the injection mixture, one which enters the interstitial space but does not enter the tissue cells. The reference substances are chosen so that, as closely as possible, they are carried in the blood stream in the same way as the substance of interest.

The anatomical structure within which the events of exchange and metabolism take place is a tissue or organ. The microcirculatory pathways in this structure consist of small-in-diameter long capillaries, more or less anastomosing, situated between tissue cells, which are surrounded by an interstitial space. In highly metabolically active organs, the microcirculation tends to be densely packed and the intercapillary distances are small; in poorly metabolizing tissues, intercapillary

distances can be much larger. In the former case, diffusion gradients can be essentially flat; in the latter case, gradients can be well developed.

Two general approaches have been taken to obtaining information from tracer studies: a stochastic one, in which model-independent parameters are derived, describing the data; a model-dependent one, in which the detailed events underlying the processing of the study substance are included in the description. The stochastic descriptions are described in Chapter 11; here we focus on combining the knowledge of the anatomy with the observations on kinetic events.

16-2. The Multiple-Indicator Dilution (MID) experiment

Each experiment must be defined to serve a particular purpose. The MID experiment is strongest and most accurately interpretable with respect to physiological events which occur close to the capillary, i.e., for capillary permeability and intraendothelial reactions. Reactions which occur in the parenchymal cells of organs are masked to some extent behind the intervening processes of penetration of the capillary wall or endothelial reactions. When endothelial permeabilities are high and when intraendothelial reactions are negligible, then the estimation of parameters governing parenchymal events is least influenced. A conceptual diagram of the capillary-tissue exchange unit, the basis for a mathematical model, is shown in Fig. 16-1. See Chapter 7 for the development of the equations and the application to data analysis.

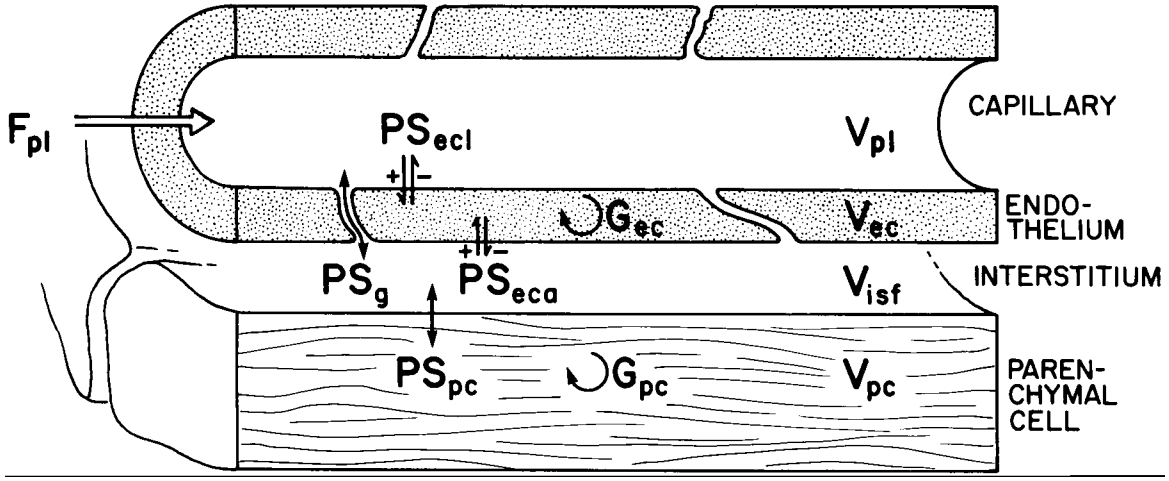

Figure 16-1: Representation of model used for analysis of indicator-dilution curves. F_{plasma}, plasma (perfusate) flow; *PS*, permeability-surface areas for adenosine passage through endothelial cell luminal membrane (PS_{ecl}); water-filled channels between endothelial cells (PS_g); endothelial cell abluminal membrane (PS_{eca}); and parenchymal cell membrane (PS_{pc}). *G*, intracellular consumption (metabolism) of adenosine by endothelial cells (G_{ec}) or by parenchymal cells (G_{pc}). *V*, volume of plasma (V_{plasma}), endothelial cell (V_{pc}), interstitial (V_{isf}) and parenchymal cell (V_{pc}) spaces. (Figure from Gorman et al., 1986.)

In order to obtain measures of the influencing processes as directly as possible and to minimize the influences of indeterminacy of these processes on the parameter of particular interest, the MID technique is based on the principle of obtaining multiple simultaneous sets of data that relate to the behavior of the solute under study. Thus, for example, if one wishes to

determine the capillary permeability of a solute, then the relevant reference solute is one which does not escape, to any significant extent, from the capillary blood during single transcapillary passage, e.g., albumin as the reference solute to determine the capillary permeability to sucrose. In this situation the albumin transport characteristics within the vascular space may be assumed to be the same as those of the sucrose; thus the shape of the albumin impulse response curve accounts for transport through the convective region, by flow, eddies and mixing, and by dispersion through a network of serial/parallel vessels between inflow and outflow. For sucrose then, an extracellular tracer, the same information is used, and the only additional information to be provided from the sucrose independently of the albumin is the capillary PS and the interstitial volume of distribution.

The difference between the intravascular indicator and the permeating one is usefully expressed as an extraction. See Fig. 16-2. The instantaneous extraction $E(t)$ is a measure of the fraction of the permeant indicator which escapes, and thereby can provide a measure of the rate of escape across the capillary wall:

$$E(t) = 1 - h_D(t)/h_R(t). \tag{16-1}$$

Its equivalent can be calculated from the slopes of the residue functions:

$$E'(t) = 1 - dR_D(t)/dR_R(t). \tag{16-2}$$

A net extraction which represents the cumulative difference between flux into tissue and return flux from tissue to blood can be taken directly from the residue curves without calculating the derivatives used in Eq. 16-2:

$$E'_{net}(t) = \frac{R_D(t) - R_R(t)}{1 - R_R(t)}. \tag{16-3}$$

Putting aside the fact that the capillaries are fed by arteries and arterioles and drained by venules and veins, one can diagram capillary-tissue regions as in Fig. 16-1. If there is efflux but no return flux from the interstitial space into the capillary lumen, then Christian Bohr's (1909) conceptual model is suitable for analysis of the indicator dilution curves, as proposed by Renkin (1959) for the arteriovenous extraction of a constant infusion of tracer potassium and by Crone (1963) using pulse injection and calculating the instantaneous extraction $E(t)$. The relevant expression considers the loss of the permeant tracer across a single barrier and is that developed by Bohr (1909), expressed in modern terminology:

$$PS_g = F_s \log_e(1 - E), \tag{16-4}$$

where PS_g is the capillary permeability-surface area product, milliliters per gram per minute, F_s is the flow of solute containing perfusate, milliliters per gram per minute, assuming uniformity of flow throughout the organ and adequacy of single capillary modeling, and E is an extraction relative to the intravascular tracer, assuming that it is due solely to unidirectional flux of tracer from blood into tissue. The implicit assumption is that the interstitial concentration of the permeating solute remains at zero, which could occur if the interstitial volume were infinite and

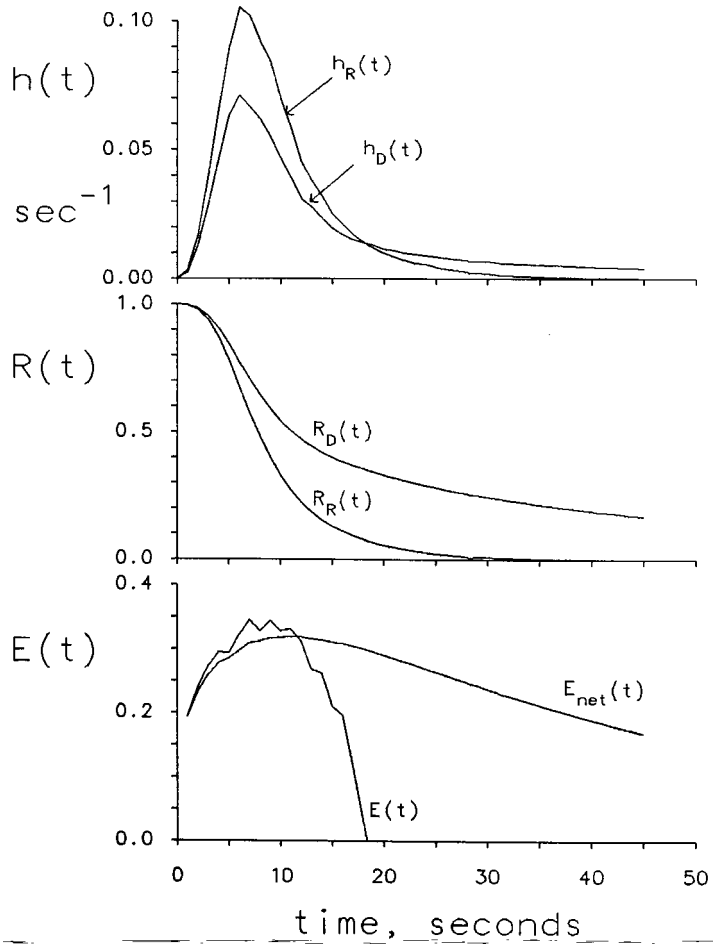

Figure 16-2: Multiple indicator dilution curves. *Top:* Following injection into the left main coronary artery, outflow dilution curves were obtained by sampling at one-second intervals from dog coronary sinus for an intravascular reference indicator, ^{131}I-labeled albumin, providing $h_R(t)$, and a permeating inert hydrophilic molecule which does not enter cells, [^{14}C]sucrose, providing $h_D(t)$. The subscript R is for intravascular reference and D for diffusible (or permeating) indicators. *Middle:* From the $h(t)$ values, the transport functions, one can calculate $R(t)$, residue function, giving $R_D(t)$ and $R_R(t)$. *Bottom:* The difference between $h_D(t)$ and $h_R(t)$ can be expressed as an instantaneous extraction $E(t)$, and the difference between $R_D(t)$ and $R_R(t)$ as a net extraction $E_{net}(t)$. (Figure from Bassingthwaighte and Goresky, 1984.)

the interstitial diffusivity high, or if the indicator became bound rapidly at extravascular sites. Crone (1963) recognized that these idealized conditions did not hold and proposed that the E in Eq. 16-1 be taken from the first few seconds of the outflow dilution curves when the interstitial concentration is nearly zero. If it were not for the heterogeneity of regional flows in an organ this technique would work quite well for solutes of low permeability, when the ratio PS_c/F_s is low, efflux is small, and return flux is slow. Nowadays one can account for the return flux, using fully developed mathematical models of the system diagrammed in Fig. 16-1 (e.g., Bassingthwaighte, Wang and Chan, 1989) and thereby improve the accuracy of the estimates of PS.

A second example: When the goal is to estimate the permeability of the endothelial luminal surface to a solute, the two references are desired, one intravascular as before, and a second one which permeates through the clefts between endothelial cells but does not enter cells, like sucrose. Ideally, this second reference substance should not enter cells, i.e., is an extracellular reference, and should penetrate the interendothelial clefts with exactly the same ease as does the solute under study. An example is to use sucrose as the extracellular reference solute for studies of adenosine uptake by endothelial cells (Schwartz et al., 1997) because sucrose has a molecular size, aqueous diffusion coefficient, degree of hydrophilicity, and charge quite similar to that of adenosine, and therefore is taken to have almost the same cleft PS_g as does adenosine. Thus if the fraction of adenosine permeating the interendothelial clefts can be inferred accurately by reference to sucrose, then the remainder of its transcapillary extraction must be explained by either binding to endothelial surfaces or by transport across the endothelial luminal surface membrane. (There seems to be no evidence for surface binding. In the dog virtually all of the adenosine, which is 98 or 99% extracted during single passage through the coronary circulation, is metabolized (Kroll et al., 1997), and must therefore have been transported across cell walls or metabolized extracellularly.) Thus by use of the sucrose reference, the endothelial PS_{ecl} is inferred accurately by

$$PS_{ecl}(\text{Ado}) \;=\; PS_{cap}(\text{Ado}) - 1.12 \cdot PS_{g}(\text{sucrose}), \tag{16-5}$$

where the 1.12 is the ratio of the free diffusion coefficient of adenosine divided by that for sucrose, to account for their difference in molecular diffusivities. (Sucrose is not a perfect reference; if the extracellular reference solute had the same diffusion coefficient as adenosine the factor would be 1.00 instead of 1.12.) The second parameter with a value that should be equal to that for adenosine is the interstitial volume, V'_{isf}.

A third reference tracer is desirable when the solute of interest undergoes facilitated or passive diffusional transport across a membrane and then undergoes intracellular reactions. The third reference solute is one which has the same extracellular behavior (cleft permeation, interstitial volume of distribution, and intravascular transport characteristics) as adenosine, and uses the same transporter across the cell wall (and has the same apparent affinity and transport conductance), but does not react inside the cell. For adenosine there is such a solute, O-methyl adenosine. Dilution curves from O-methyl adenosine should therefore provide evidence on parameter values for PS_{pc} and for V'_{pc}, independent of the data from adenosine but equivalent in value. (This has not yet been firmly established, but is likely.) This third reference therefore supplies PS_{pc} and V'_{pc} for adenosine, given that the premises are verified experimentally.

Table 16-1: Reference tracers

Solute class	Information provided on solute under study
Intravascular	Convective delay and dispersion in all vessels perfused
Extracellular	Cleft *PS*, PS_g, and interstitial volume, V'_{isf}
Unreacted but transported analog	Cell *PS*, PS_{pc}, and intracellular volume of distribution, V'_{pc}

16-2.1. Data acquisition in the MID experiment

For the study of tracer transport and metabolism in an organ with a single inflow and a single outflow, the most explicit information is obtained with the multiple-indicator dilution technique, injecting a set of tracer-labeled solutes simultaneously. By this approach it is certain that the intravascular transit times, arterial and venous, are identical for all the solutes. (Unless there is entry of the permeating solute into red blood cells, and a consequent "red cell carriage effect," whereby the fraction carried by RBC has a higher velocity than does the fraction carried in the plasma and there is a reduction in the rate of escape from the capillary because of the relative unavailability of the RBC fraction.) With radioactive tracers the relative amounts of radioactivity chosen for each solute depend on the methods of analysis of the samples. Often with organic solutes it is easiest and most accurate to use three β-emitters together; ^{131}I, ^{14}C, and ^{3}H are a commonly used since they can be attached to a wide variety of solutes and can be distinguished by liquid scintillation counting without any preceding chemical separation (Bukowski et al., 1992). When four or five tracers are being used simultaneously then either physicochemical separation will be needed, e.g., by HPLC, or combinations of gamma- and beta-emitting tracers should be used (e.g., Goresky, 1963).

A diagram of the experimental setup for examining the reactions involving the transformation of hypoxanthine to xanthine to uric acid in the isolated perfused guinea pig heart is shown in Fig. 16-3.

The set of tracers are injected simultaneously as a compact bolus into the inflow to the organ, attempting to provide mixing of the bolus of fluid with the perfusate so that it is thorough and complete. If mixing is not complete before the first branchpoints in the arterial system, then different parts of the organ would receive tracer doses out of proportion to the fraction of flow, and would therefore be misrepresented in the outflow. If a disproportionately large fraction of the dose entered a particular region, then the characteristics of this region bias the results of the interpretation of the analysis of the outflow dilution curves. In theory, the fraction of the dose entering each element of the fluid at the injection site should be in exact proportion to the fraction of flow through that element. This is flow-proportional labelling (Gonzalez-Fernandez, 1962). It is virtually impossible to achieve this exactly, but the proportion is reasonably well approximated if there is adequate mixing by disturbances in the flow patterns before the branchings occur. (In contrast, cross-sectional mixing is clearly undesirable: simply labelling a cross-section of the fluid stream as if by inserting a cylinder of tracer-labelled fluid into the column of fluid at the entrance to the system creates equal labelling of the infinitely slow laminae at the wall of the vessel with the highest flow laminae at the center of the stream; this creates a striking bias or weighting of the peripheral laminae; in theory the layer at the wall, which is not moving, should contain no label.

Data is normally acquired by sampling the outflow. In isolated organ systems the outflow from the whole organ is collected in a series of timed collections. The essential information is the time of beginning each collection, the time of ending, and the volume of the sample. For studies of the heart, samples are collected at 1 or 2 second intervals for the first 30 seconds and with gradually diminishing frequency thereafter. Nowadays, with computer-controlled sampling, we spread out the length of the collection periods gradually so that when the shapes of the outflow curves are changing gradually there are fewer samples. The idea, very roughly, is that in order to minimize the work of chemical analysis on the samples, fewer samples are needed when the concentrations of the tracers are changing only slowly. The sample volume per unit time is also a measure of the flow during the period of obtaining the samples.

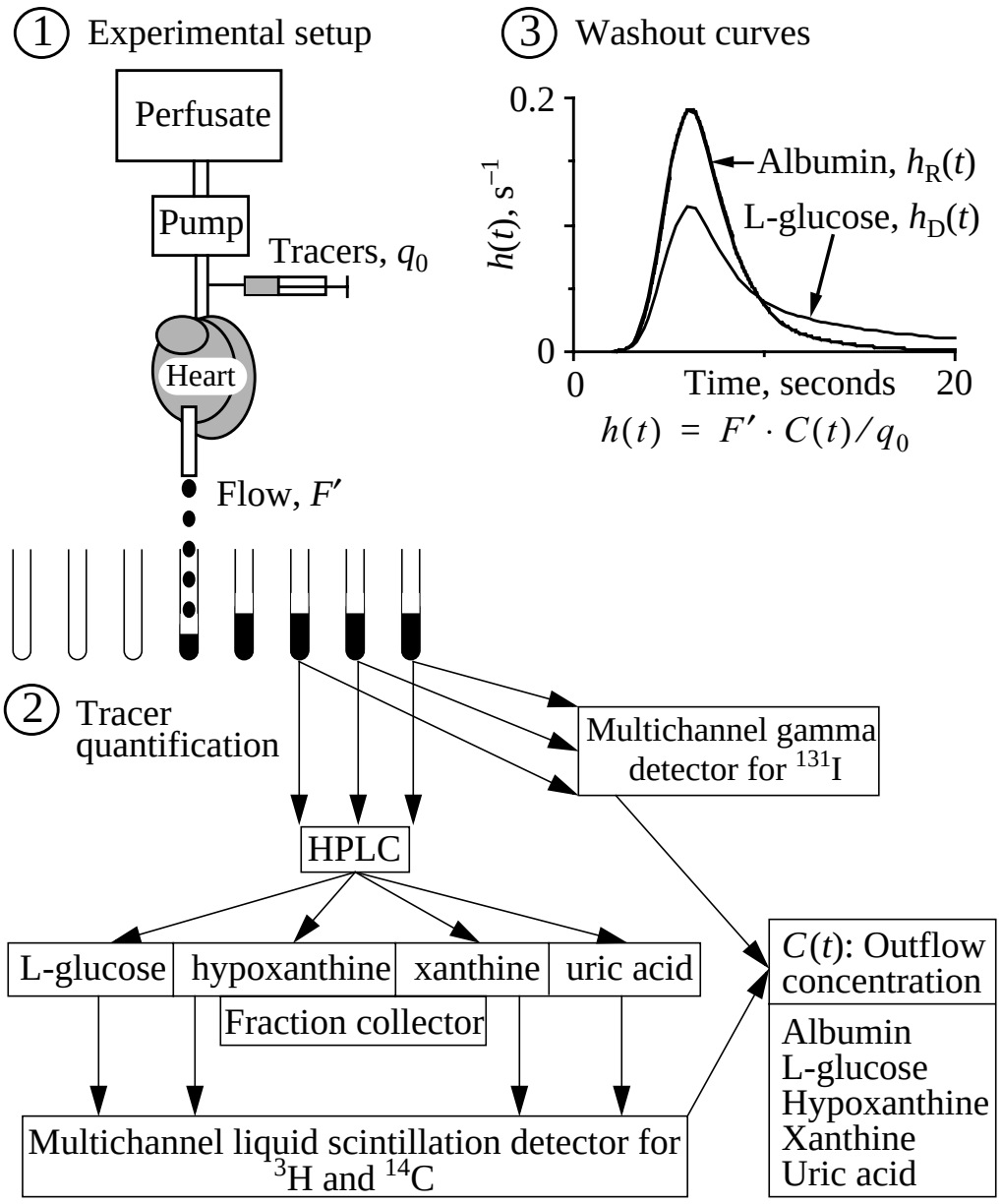

Figure 16-3: Schematic overview of procedures underlying the application of the multiple-indicator dilution technique to investigation of multiple metabolites. Following a bolus injection (within a half second) of a set of tracer-labelled solutes into the inflow, in this case of an isolated perfused heart, samples of the effluent are taken at brief time intervals (e.g. 1/second). The samples are split, analyzed first for the activity levels of ^{131}I-albumin (the intravascular indicator in this case) using a gamma scintillation counter, and then analyzed using HPLC (high performance liquid chromatography) to separate the chemical constituents and then quantitated for the levels of the beta-emitters tritium (^{3}H-L-glucose, the extracellular marker) and of ^{14}C-carbon in the form of the originally injected hypoxanthine and its metabolic degradation products xanthine and uric acid. A typical pair of albumin and glucose outflow dilution curves are above.

16-2.2. Normalization of the indicator dilution curves to fraction of dose

The concentration-time curves obtained must be normalized to the "fraction of dose emerging" either per unit volume of outflow or per unit time. We prefer the latter for this puts it into the framework directly defined by the differential equations. To do this the calibration of the dose injected is critical. Because the tracer concentrations in the injectate are high, precluding isotope counting on accurately measurable volumes of aliquots of the injectate solution, serial dilutions are normally required. We normally determine the activity of 10 to 20 aliquots, at several different dilutions, attempting to obtain something better than 1% accuracy in the estimates of the dose. This allows normalization to the unit response, h(t), the fraction of dose per second emerging with the outflow:

$$h(t) = \frac{F \cdot C_{\text{out}}(t)}{q_0}. \tag{16-6}$$

This normalized outflow response is not identical to the formal impulse response of the system for two reasons: one is that the input function is not usually a Dirac delta function, an infinitely thin spike at t = 0, but is more spread out due to finite duration of the injection itself and to physical spread of the injectate in the volume of perfusate in the inflow tubing or blood vessels due to the force of the injection, a jet effect. Nevertheless, since the injectate form should be identical for all of the tracers within the injection syringe, direct comparisons can be made between the several tracers using the mathematical models, given that one has a close approximation to the input function.

16-2.3. Dose calibration

The calibration of the injected dose is not easy. To do this we take 20 aliquots of the injectate solution, using a few different dilutions that are compatible with the radioactivity levels that can be assessed by the gamma or beta scintillation counting methods being used. These samples contain all of the tracers being used, and therefore the samples must be put through the same set of separation and counting processes as are applied to each sample. From these 20 samples we obtain 20 estimates for the dose of each of the tracers injected.

In addition, samples of each of the tracers that were used to make up the dose are assessed separately and individually. This is done in order to provide an additional check on the amounts put into the dose on samples in which there is only one tracer and no inaccuracy introduced by spillover corrections which enlarge the statistical error (and even sometimes bias) in the assessment of the dose. All this is to get the estimates of the dose, and thereby the fraction of dose per sample or per unit outflow volume, which sounds pretty tedious, and it is, but the other side of the coin is that the measure of the dose and the volumes of the outflow samples are the two least accurate measures that one makes in the indicator dilution technique, and therefore require this level of repeated measurement to gain the needed accuracy.

16-2.4. Recording the input function

Since no separation of the various tracers occurs before the bolus enters a region where interactions with elements of the biological systems occur, the recording of any one of the input tracer concentration-time curves provides exact information on the whole set. This has the great advantage of reducing sources of error and allows one to get the best possible estimates of the

transport functions of the system. Having an optically labelled indicator is a cheap and effective way of getting the input function, by taking a small sampling stream from the inflow tubing through a densitometer. In those conditions where the total inflow is small, as in experiments where one is perfusing a small organ, an albumin dye marker such as indocyanine green (Fox et al, 1957; Bassingthwaighte et al, 1964 #10015) the whole of the inflow can go through the densitometer to give the input function, as was done by Deussen and Bassingthwaighte (1996) and Harris et al., 1990).

Given an input function, $C_{in}(t)$, one can analyze the data in a "forward" fashion in the time domain, using $C_{in}(t)$ directly as the input to the model function. The procedure is in principle the same when one uses an analytical equation describing the model impulse response or uses a numerical model. In the former case one uses the convolution integration to obtain an *estimate* of the outflow dilution curve, $C'_{out}(t)$:

$$C'_{out} = C_{in} \otimes h(t), \tag{16-7}$$

where the $\otimes$ denotes the convolution integration. Then the parameters of the model for h(t) are optimized through an iterative routine to obtain a best fit of $C'_{out}(t)$ to the observed data curve, $C_{out}(t)$, minimizing the least squares distances between these. When the model is the solution to a set of time domain equations, then $C_{in}(t)$ serves to provide the concentration values at each point in time and the model outflow is $C'_{out}(t)$, and the parameters of h(t) optimized. This avoids the optimization, which is computationally costly, and is faster to compute if the model is not too complex. In this method the least squares uses the distance between the data and the model output at each data point; since the error in the data point is known, the residual errors can be evaluated in that light, and examined for systematic variations.

An alternative approach is to take advantage of the potential efficiency of transform techniques. For example using frequency domain transforms, $H(\omega)$, the Fourier transform of h(t), and the Fourier transfroms of the observed $C_{in}(t)$, and the observed $C_{out}(t)$, which we'll label in bold font $\boldsymbol{C}_{\mathbf{in}}(\omega)$ and $\boldsymbol{C}_{\mathbf{out}}(\omega)$, then one has an algebraic calculation (at each frequency) to replace the convolution integration:

$$\boldsymbol{C}'_{out}(\omega) = \boldsymbol{C}_{in}(\omega) \cdot \boldsymbol{H}(\omega). \tag{16-8}$$

The optimization requires the fitting of $\boldsymbol{C'}_{\mathbf{out}}(\omega)$ to $\boldsymbol{C}_{\mathbf{out}}(\omega)$ in the frequency domain, so unless a carefully weighted least squares algorithm is used, the influence of the errors is quite different from that obtained experimentally. A check on the influence of such erroneous weighting is to convert all the curves back into time domain and plot them, and to show the residuals, the distances $C'_{out}(t) - C_{out}(t)$, or the squares of these at each time point, again looking for systematic misfitting. Remember that an even weighting of the points in the time domain is transformed into a reciprocal time weighting in the frequency domain. This can work out reasonably, especially in those cases where there is maximum information in the early parts of the outflow curve and then a relatively slow more or less exponential washout at the tail at long times.

16-2.5. Multiple data sets

The most power in the analysis is gained when one has available the maximum amount of simultaneously-acquired, self-consistent data. Thus one needs to obtain along with the largest practical set of indicator dilution curves the full set of experimental data. Flow, temperature, pH,

pCO_2, pO_2, etc. will be important in defining the physiological status of the preparations. So will the organ weight, water content, the functional performance of the organ, and the concentrations of solutes and substrates in its venous effluent.

In multiple-indicator dilution experiments the idea is to obtain information on the whole of the set of solutes simultaneously, as described above. When the choices of reference solutes include an intravascular reference, an extracellular solute matched in cleft permeability to the prime permeating solute, and a solute that is transported like the prime permeating solute but which is not metabolized intracellularly, then we have a matched set. This is not a universally defined set, for there will be situations in which there is extracellular metabolism, for example by a phosphatase, so the matching is specific for the prime substrate only.

16-3. The analysis of MID data sets

16-3.1. Conservation principles

The general theory outlined at the beginning of the chapter needs to be applied to each tracer in a multiple-indicator dilution study. It is usually not too difficult to determine the fractional recovery of the inert, nonreactive reference intravascular and extracellular indicators. For any tracer-labelled substrate that undergoes transforming reactions, the tests for conservation require finding all of the tracer no matter what chemical form it may have taken. For ^{14}C-glucose one must find its fractional storage (as glycogen, fat, protein, etc.). Thus many experiments require chemical and isotopic analysis of the sequence of outflow samples, and also the same analysis of the whole organ. The latter exercise is particularly expensive and tedious, given the known heterogeneity of flows and metabolic functions. See the chapter of this book by van Beek et al. with respect to metabolic heterogeneity.

16-3.2. Residue plus outflow data

Residue function data are not often available simultaneously with outflow dilution data. The exceptions are imaging studies where one may have residue data by positron emission tomography, single photon emission computed tomography, coincidence detection of positron emitters from the whole organ, single photon residue detection, X-ray computed tomography, or magnetic resonance contrast signals.

Residue data are particularly valuable when the retention of tracer within the organ is prolonged: in this case the outflow concentrations are low, difficult to measure, and therefore their integrals are not as accurate as is desired. Having both outflow and residue is ideal from the mass balance point of view:

$$\int_0^t h(\lambda)d\lambda + R(t) \;=\; 1.0\,, \tag{16-9}$$

which is to say that at time t the total dose is to be found as the sum of the outflow to that time, plus the residue at that time. An example of this approach applied to estimation of myocardial oxygen consumption from ^{15}O-oxygen input, residue and output curves is provided by Deussen and Bassingthwaighte (1996).

16-4. Integrated analysis of different data sets acquired in a single study

The power of the multiple-indicator dilution method is in the combining of information of several different types, gathered more or less simultaneously, into a common data set for which a complete and self-consistent explanation should be found. The "explanation" is an analysis which accounts for the full set of information, which is quantitative and physiologically realistic, and which provides estimates of parameter values and confidence limits on the estimates. If one has only a single indicator dilution curve consisting of 30 to 50 points and a complex model to fit to these data, then the fit may not be well-determined: there may be too many different sets of parameters which will fit the single curve equally well. The more complex the model the more data are needed to refine and constrain the estimates of the parameters.

The standard multiple-indicator dilution study is ordinarily designed to obtain information on three tracers simultaneously, an intravascular reference tracer, an extracellular reference tracer having an extracellular volume of distribution similar to that of the test solute, and the test solute itself. Can more be done? The answer is clear: the more information that can be gathered on the status of the organ at the time of the experiment the clearer and more definitive will be the results of the analysis. By the same token, information which may not be quite simultaneous, but which can be reasonably considered to be applicable to the status at the time of the indicator dilution curves is really invaluable.

In an intact organ there is inevitably some considerable heterogeneity of flow. Very often for studies of the myocardial tracer exchanges we have assumed that information acquired on other hearts at other times is applicable to the particular study. The assumption is based on the oft-repeated observation that the heterogeneity of flows in the myocardium is very much the same from heart to heart and is stable in the same heart from one time to another. If this is really true then we would not have to measure the flow heterogeneity, except occasionally as a check. This is probably true, not only because the heterogeneity doesn't change very much, but also because small changes in heterogeneity have a negligible influence on the estimates of the parameters of interest, the permeabilities and the reaction rates of the solutes. But one cannot count on this if the physiological conditions are abnormal or are being manipulated. For example, when combinations of drugs are used to change vasomotion or influence metabolism, then the regional flows should be determined using microsphere distributions in the same experiment. Likewise one may need to determine the volumes of distribution for the vascular and extracellular solutes and for the water content of the tissue samples, all in the interest of reducing the degrees of freedom for the analysis which follows using particular models. When one needs to model local metabolism from tissue samples, then it becomes essential to have a measure of the flow in each of those samples.

The desired information set therefore consists of $w(f)$, the probability density function of regional tissue flows (ml per g per unit time), the regional volumes of distribution for the vascular, extracellular and water markers (and sometimes others, for example markers of intracellular binding spaces), as well as the dilution curves, $h_R(t)$, $h_E(t)$, and $h_D(t)$, and in certain cases a second permeating marker, $h_{D2}(t)$, one which permeates the cell but is not metabolized.

For linear systems this is often enough. But the fact is that systems are seldom linear in biology. For tracer levels of a solute the transporter or the enzyme assisting its reaction are operating in their linear range, far below the levels at which they become more than a tiny fraction bound by the available solute. Concentrations are such that a substantial fraction of the transporter or enzyme molecules are occupied. To test for this, one needs to repeat the experiment with

different ambient concentrations of the substrate. Normally one can only raise these levels, so that is the experiment to do: repeat the MID study at two or three different levels of the substrate to determine whether or not the apparent behavior changes. The expectation is that if it is near saturation of the transporter or enzyme, then raising the concentration will reduce the fraction which is transported or reacted.

A way of testing this idea efficiently was introduced by Linehan, Dawson and colleagues in a series of studies in the early 1980's, the so-called "bolus sweep" technique (Rickaby et al., 1981; Malcorps et al., 1984). It was so designated by Bassingthwaighte and Goresky (1984) in recognition of its power, namely the power to estimate the transport rate for the substrate in its passage across a membrane at a variety of different concentrations within a few seconds. The technique was simply to add to the tracer in the injectate a known amount of the mother substance (the substance for which the tracer is the marker, e.g., a few millimoles of glucose added to the chemically insignificant few microcuries of radioactive glucose). As the bolus enters the exchange regions its initial part has a very low concentration of mother substance, therefore the tracer has full access to the transporter. A few moments later as the chemical concentration of the substrate in the bolus rises towards its peak level, it exerts more and more competition for the transport sites, and so reduces the effective fractional transport of the tracer. After the peak, the nontracer chemical mother substrate concentration again falls and lessens the competition for the tracer, and the effective transport rate again rises. (See Chapter by Linehan et al.) The nice physiological result of this approach is that one can test the behavior of a substance that has marked biological effects if given as a steady concentration into the inflow; by giving it so transiently, large pharmacological responses are avoided and the parameter values represent those in the more physiological situation.

16-4.1. Reactants and products

Even better than having a set of independent tracers is having a set which are intimately related, not only by parallels in molecular behavior, but also by having one give rise to another, a set of substrates and metabolites related by being in a sequence or particular arrangement of reactions. This situation is the focus of Chapter 7, by Bassingthwaighte et al. Such combinations provide for a series of checks and balances, for example, the amount of a substrate reacted should be the same as the amount of products formed in the reaction.

A further independent check is provided by steady-state measurements of chemical arteriovenous differences in the same preparation and at the same time as the tracer transient information is obtained. When tracer glucose extraction is measured by the multiple-indicator dilution technique the peak instantaneous extractions in the brain (Crone, 1963) and the heart (Yipintsoi et al., 1970; Kuikka et al., 1986) are high, 50% or so, but the arteriovenous differences are small, less than 10% in the brain and only 2 or 3% in the heart. Why should these be so different when the tracer ^{14}C-glucose is chosen to have the same molecular characteristics as the "mother substance," the chemical glucose? The answer is simply that the tracer extraction compared to the reference intravascular tracer reflects the unidirectional fluxes, more or less, across the capillary membrane, and provides a measure of the fraction which escapes, transiently, from the blood into the extravascular tissue. In contrast, the arteriovenous difference in chemical concentrations represents the net loss of material, glucose, into some other form (lactate or carbon dioxide); this is a net flux due to a loss or transformation of material. The net fluxes are always much less than the unidirectional tracer fluxes; if glucose consumption were zero, the net A-V difference would be zero, but the tracer transient would still be about 50% extracted.

16-5. Whole organ modeling

For the analysis of signals obtained by external detection techniques such as positron tomographic imaging, PET, magnetic resonance imaging, MRI, and X-ray computed tomography, X-ray CT, investigators and diagnosticians usually obtain a sequence of images. For physiological interpretation in terms of the underlying physical and chemical events, it is essential to use models when one wants to learn more than the simplest measures. Among simplest measures one can often include volume and flow estimates, but not always, for it commonly occurs that the distinctive estimation of these two parameters simultaneously requires using knowledge of the anatomy or of other properties of the tissue. The two most accessible measures of indicator transport are the areas under dilution curves and their mean transit times following a pulse injection. Mass conservation for substances which are not destroyed, such as radioactive tracers, relies on the general expression:

$$\text{Tissue content} = \text{What has come in} - \text{what has gone out, or}$$

$$q(t) = F\int_0^t C_{\text{in}}dt - F\int_0^t C_{\text{out}}dt,$$

where $q(t)$ represents the mass of indicator in the tissue at time t, F is the flow of indicator-containing fluid and $C_{\text{in}}(t)$ and $C_{\text{out}}(t)$ represent the concentration-time curves for the indicator at the inflow and outflow. Such expressions represent whole organ behavior exactly when the organ is supplied by a single artery and drained by a single vein. When there are multiple inlets and multiple outlets then the first term on the right is replaced by a sum of similar terms for each inlet, and likewise the second term on the right is replaced by a similar sum of the outputs (Lassen and Perl, 1979). When the input is a brief pulse input, theoretically infinitely short, then $C_{\text{in}}(t)$ is a scaled Dirac delta function, $q_0\delta(t)/F$, where q_0 is the dose of indicator injected and $C_{\text{out}}(t)$ is $q_0h(t)/F$, where $h(t)$ is defined as the impulse response or transport function of the organ. See the Introductory Chapter and the general overview by Bassingthwaighte and Goresky (1984). This expression defines a basis for using the principle of conservation of mass to be applied as a check in the analysis. To this point the approach is not dependent on any model. Such an equation can be used for the "model-free" estimation of flow, for example,

$$F = q_0 / \int_0^\infty C_{\text{out}}dt$$

which is true even when the input is dispersed, with the proviso that the indicator has passed through the system only once, i.e., there is no recirculation.

Another conservation statement, also model-free, is for the mean transit time volume, V', of the system:

$$V' = F \cdot \bar{t}$$

where the mean transit time $\bar{t}$ is the first moment of the impulse response. But to model a whole organ and obtain estimates of parameters of the permeabilities and reaction rates one must make some basic assumptions about the structures or arrangements of the components of the organ. There are several reasons for this. If a substrate undergoes a reaction to form a product and the

form of $C_{out}(t)$ for the product differs from that of the substrate, then the two molecules must have undergone different transport or other processes in travelling from the reaction site to the outflow. These might be due to differing membrane permeabilities, different solubilities or volumes of dilution, different degrees of binding, or differences in diffusivity. All of these require interpretation in terms of structure-function relationships.

Assumption 1. There is no net exchange of indicator between neighboring capillary-tissue units. This appears to be justified for a wide range of small hydrophilic solutes (Goresky, 1963; Bassingthwaighte, 1970; Kuikka et al 1986). Consequently we view the organ as consisting of parallel independent pathways, each differing from the others only with respect to the local flow, as in Fig. 16-4.

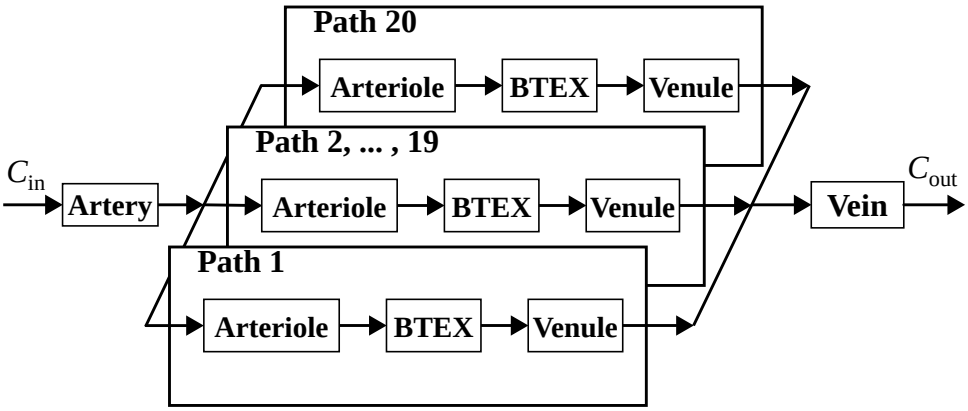

Figure 16-4: A twenty-path multicapillary model for blood-tissue exchange in a whole organ. The model consists of single common entrance and exit vessels, a large artery and a large vein, and a set of parallel independent units having differing flows, each unit consisting of an arteriole, a capillary-tissue exchange unit and a venule. All of the components of the system are dispersive, i.e., their impulse responses show a spread of transit times through passage from entrance to exit.

To characterize this model in a computable form one now has to define several variables. These fall into groups:

1. The description of the probability density function of regional flows, $w(f)$, as defined in Chapter 1, and how to represent it in the model: the regression as a finite number of pathways requires care to avoid numerical inaccuracy. King et al. (1996) provide algorithms to select good approximations to $w(f)$ by histograms of $N \leq 20$.
2. The descriptions of transport through the large and medium-sized vessels: simple linear operators (King et al., 1993) have proven useful in describing intravascular dispersion and delay.
3. The descriptions of the exchange units: these are described next.

16-6. A basic blood-tissue exchange unit.

Beginning with Christian Bohr's (1909) demonstration that the concentration of a solute escaping from a long tube should diminish exponentially as a function of distance from the entry to the

tube, there has been a continuing development of mathematical models of the exchange processes between the blood in a capillary and the fluid in the surrounding tissue. Early models used compartmental analysis with one instantaneously mixed compartment representing the blood (or plasma) space and a second representing all the extravascular tissue space, e.g., Sapirstein (1958). Through the years, the modeling of blood–tissue exchange has evolved in several ways: additional anatomical regions (e.g., endothelial and parenchymal cells) are now included, distributed models that can exhibit axial (i.e., arterial to venous) concentration gradients and describe the axial diffusion which dissipates the gradients have been developed, and analytical and numerical techniques have been improved so as to increase both accuracy and computational speed.

Sangren and Sheppard (1953) first gave the analytic solution for a blood–tissue exchange model containing two regions, capillary and extravascular tissue, separated by a permeable membrane. The solution assumed that axial diffusion in both regions was zero and that radial diffusion was infinitely fast. The return flux from the extravascular region to the capillary was taken into account; thus mass was conserved. Goresky, Ziegler and Bach (1970) extended this to include uptake from the ISF into the parenchymal cells, without return flux from this third region. Rose, Goresky and Bach (1977) developed a solution for the analogous model that included the parenchymal cell and its membrane, a two-barrier three-region model with return from all regions back to the capillary space. Bassingthwaighte (1974) developed a whole-organ model which accounted for dispersion in arteries and veins. This model was extended into a multicapillary model by Kuikka et al. (1986), who also added axial diffusion, and by Lumsden and Silverman (1986), who added terms for the consumption of the solute in all three regions.

We have previously described a three-barrier four-region blood–tissue exchange (BTEX) model (Bassingthwaighte, Wang and Chan, 1989) that accounts for capillary plasma, endothelial cells, interstitial fluid (ISF) and parenchymal cells, and axial diffusion and consumption in all regions. The solutions are numerical, using computationally efficient algorithms (Bassingthwaighte, Chan and Wang, 1992) that result in computational speed about 10^7 times faster than an analytical solution and provide good accuracy at long solution times even with parameter values making computation "stiff" (e.g., $PS/F > 1000$).

In order to provide generality in concept and in application, it has proven useful to work with a basic model form that allows much generality. The model form is also such that it can be reduced to a minimal model, so preserving the strengths and weaknesses of a large variety of model forms. This is MMID4, a model form which does most everything with respect to organ blood flow, diffusion, vascular transport, exchange by permeation, and tracer removal by reaction.

MMID4 is an acronym for Multiple path, Multiple tracer, Indicator Dilution, 4 region model. It is used to examine the behavior of three types of tracers: one that remains in the vasculature, one that can leave the vasculature but remains extracellular, and a fully permeant tracer that enters cells. The four regions are plasma, endothelial cells, interstitial fluid and parenchymal cells. The model can be used to study the physiology of the exchange process or as an analytical tool to help analyze actual experimental data. The exchange process may be examined by viewing the instantaneous outflow concentration, the instantaneous extraction, or the amount of indicator remaining in the exchange unit (i.e., the residue function). The model includes provisions for examining the effects of indicator delay and dispersion between the injection site and the target organ and the effects of flow heterogeneity on exchange within the organ.

The extension of these equations to a multicapillary model with a set of capillaries having different flows is discussed by Bassingthwaighte, Wang and Chan (1989). They also present the

numerical methods used to obtain solutions to these equations that are analytic within each space and time step.

MMID4 includes within each pathway the model shown in Fig. 16-5 and two reduced forms

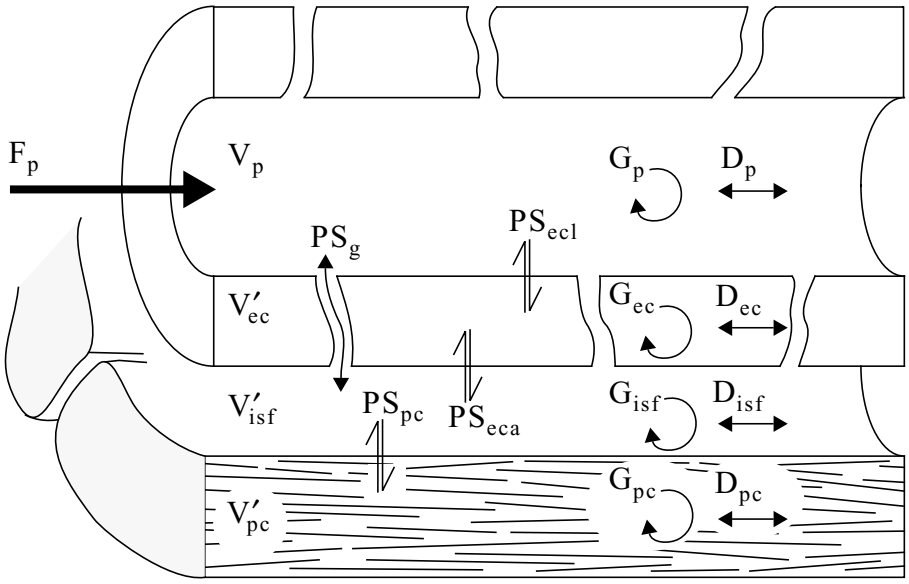

Figure 16-5: Basic blood–tissue exchange unit. Parameters affecting exchange of the permeant tracer. F_p and V_p are the same for all tracers.

of it. These reduced forms are used for modeling the “vascular” and “extracellular” reference tracers. The “vascular” model permits both intravascular and an “interstitial” region, seldom used but available to account for leakage or presence of a receptor on endothelial cells. The extracellular reference solute chosen is normally one with the same permeability through the clefts between endothelial cells and the same V_{isf} as the permeant tracer targeted in the study. The use of these “in-built” controls reduces greatly the number of free parameters for the permeant sought in the optimization to fit data. The plasma flow, F_p, the plasma volume, V_p, the flow heterogeneity and the intravascular dispersion are the same for all tracers.

Exchange units in the model are arranged in a number of parallel flow pathways. Before entering these pathways, the flow passes through a large vessel component. Each flow pathway consists of a small vessel in series with a blood–tissue exchange unit that encompasses the parameters shown in Chapter 1. Including the large and small vessel components provides a means of accounting for delay and dispersion of the indicator between the injection site, the organ, and the outflow. The parameters governing large and small vessel behavior are the volume of the vessels and a parameter defining the degree of delay and dispersion that the input function incurs before reaching the exchange unit.

Flow heterogeneity in the target organ is taken into account by making a number of parallel pathways available to the tracers and defining the flow distribution, $w(f)$, through the pathways. MMID4 can be used with up to 20 pathways.

While this BTEX model permitted the consumption of the solute in any region, the solute consumed in a region undergoes no further convection or diffusion. The amount consumed may

be considered to either disappear from the system or, since that quantity is calculated by the model, it may be considered to be sequestered in the region in which it was consumed. The former is appropriate for a tracer undergoing radioactive decay and the latter for a tracer such as deoxyglucose that undergoes only the first step of glucose metabolism and then is trapped within the cell. Neither of these is, however, appropriate for a solute that undergoes a metabolic transformation that produces a product that can diffuse, or be transported, back out of the cell or that may be further metabolized to produce a diffusible product.

Consider the case of ^{14}C-labeled adenosine. Wangler et al. (1989) have shown that tracer adenosine injected into the inflow of the isolated guinea pig or rabbit heart is metabolized during its single transit of the microvasculature. When the metabolites in the outflow samples are separated by HPLC, the label appears not only on adenosine but also on its metabolites inosine, xanthine, hypoxanthine, and uric acid. The appropriate model for this situation is one in which solute reacts to form a product which is really the input to a model for the product with its own set of parameters governing its exchange processes. For adenosine and its products, a sequence of such interrelated models is required. This is described next as MSID4.

16-7. A whole-organ model, MSID4, for a reactant/product sequence

Our purpose here is to present a multi-solute, three-barrier, four-region, axially-distributed model for blood–tissue exchange that accounts for convection along the capillary and exchanges, across permeable membranes and through the inter-endothelial cell gaps between endothelial cells, ISF, and parenchymal cells. Reactions leading to both sequestration and production of a metabolite are permitted in all regions within cells or extracellular spaces; the consumption of tracer-labeled substrate is considered to be a linear process. A fraction goes into forming a metabolite that can exchange and be further metabolized and the remainder is sequestered permanently in the region in which it is formed. However, in this model no reactions are allowed to result in the return of tracer to an antecedent species, i.e., the reaction sequence is unidirectional. NOTE: In the subsequent discussion, we will use the term “metabolite” for each of the product chemical species produced from the original substrate.

This Multipath, multiSubstrate Indicator Dilution, four-region model, MSID4, is based on the MMID4 model discussed above. The arrangement of the non-exchanging vascular units has the structure shown in Fig. 16-4. However, each of the one to twenty flow paths contains a set of exchange units, one for each substrate modeled, rather than a single exchange unit for each path. Therefore, for a 20-path, 6-solute reactant-metabolite model there are 120 BTEX units plus another 20 each for the vascular reference tracer $h_R(t)$ and for the extracellular reference tracer $h_E(t)$. The probability density functions of regional flows and the parameters for intravascular transport in the large and medium size vessels are the same for all substrates. Each solute, substrate or metabolite has a separate set of parameters for the exchange unit.

A BTEX model for transport and exchange between the plasma (*p*), endothelial cells (*ec*), interstitial fluid (*isf*), and parenchymal cells (*pc*) in a single tissue-capillary unit is diagrammed in Fig. 16-4. Depending on the assumptions made, this general model can be described mathematically in a variety of ways. For the situation in which the only input to the system is by convection into the upstream end of the plasma, an explicit mathematical description is given by assuming steady plug flow in the plasma, the absence of radial (i.e., perpendicular to the direction of flow) concentration gradients in each physical region, and linearity of the coefficients for convection, diffusion, and consumption. The equations of the model account for conductances,

PS, across the barriers between the regions, the regional volumes of distribution (V'), the dispersion in the axial direction (D), and first-order consumption (G).

The equations for concentration of the tracer as a function of time, t, and the axial position along the unit, x, are, in the plasma,

$$\frac{\partial C_p}{\partial t} = -\frac{F_p L}{V_p} \cdot \frac{\partial C_p}{\partial x} - \frac{PS_g}{V_p}(C_p - C_{isf}) - \frac{PS_{ecl}}{V_p}(C_p - C_{ec}) - \frac{G_p}{V_p}C_p + D_p\frac{\partial^2 C_p}{\partial x^2}; \quad (16\text{-}10)$$

in the endothelial cells,

$$\frac{\partial C_{ec}}{\partial t} = -\frac{PS_{ecl}}{V'_{ec}}(C_{ec} - C_p) - \frac{PS_{eca}}{V'_{ec}}(C_{ec} - C_{isf}) - \frac{G_{ec}}{V'_{ec}}C_{ec} + D_{ec}\frac{\partial^2 C_{ec}}{\partial x^2}; \quad (16\text{-}11)$$

in the interstitial fluid,

$$\frac{\partial C_{isf}}{\partial t} = -\frac{PS_g}{V'_{isf}}(C_{isf} - C_p) - \frac{PS_{eca}}{V'_{isf}}(C_{isf} - C_{ec}) - \frac{PS_{pc}}{V'_{isf}}(C_{isf} - C_{pc}) - \frac{G_{isf}}{V'_{isf}}C_{isf} + D_{isf}\frac{\partial^2 C_{isf}}{\partial x^2}; \quad (16\text{-}12)$$

and in the parenchymal cells,

$$\frac{\partial C_{pc}}{\partial t} = -\frac{PS_{pc}}{V'_{pc}}(C_{pc} - C_{isf}) - \frac{G_{pc}}{V'_{pc}}C_{pc} + D_{pc}\frac{\partial^2 C_{pc}}{\partial x^2}. \quad (16\text{-}13)$$

The terms are as follows: C, concentration in moles per milliliter; PS, permeability-surface area product in ml g^{-1} s^{-1}; F, plasma flow in ml g^{-1} s^{-1}; L, capillary length in centimeters; G, regional clearance or gulosity in ml g^{-1} s^{-1}; D, axial diffusion or dispersion coefficient in cm^2 s^{-1}; V, volume in ml g^{-1}; and V', volume of distribution in a region in ml g^{-1}. A volume of distribution is the region-to-plasma partition coefficient (dimensionless) times the actual anatomic volume of the region (ml g^{-1} of tissue). Subscripts on concentrations or volumes refer to a region with the exception of the conductance across the luminal and abluminal surfaces of the endothelial cells, PS_{ecl} and PS_{eca} respectively, and the conductance through the gaps between the endothelial cells, PS_g. The existence of this direct path for plasma-isf exchange that bypasses the endothelial cells makes this model different than one with a set of concentric volumes.

16-7.1. Parameters governing tracer exchange

The parameters affecting the concentration of the permeant tracer in each region are shown in Fig. 16-5. This tracer can move to all regions, and has an apparent volume of distribution (V') in each. In the intravascular region, this is the plasma volume (V_p). For other regions, the equilibrium condition is defined by $V'_r/V_p = C_r(t = \infty)/C_p(t = \infty)$, where the subscript r indicates region, and the concentration ratio C_r/C_p shows that V'_r is a virtual volume of plasma-equivalent concentration. The tracer may be metabolized or undergo chemical reactions that result in its being cleared from the region. The degree to which this happens is indicated by the intraregional consumption or "gulosity" (G). Movement of the tracer between regions is governed by the permeability-surface

area product (PS) of the various barriers. A molecule of tracer may move, for example, between the capillary and the interstitium. Two routes are available; it can either move through the clefts between the endothelial cells, or it can move through the endothelial cell. In the first case, movement depends on one PS product (PS_g where the subscript *g* denotes gap on cleft). In the second, movement depends on two PS's, the PS product at the luminal side of the endothelial cell (PS_{ecl}) and the PS product on the abluminal side of the cell (PS_{eca}). The plasma flow affecting the permeant tracer exchange is the same flow (F_p) for all of the tracers. In formal notation, the outflow concentration-time curve seen from an exchange unit in response to an impulse input of tracer is denoted as $h(t)$ as in Chapter 1. We use $h(t)$ as a general symbol to denote the normalized (unity area) outflow dilution curve even when the input has forms other than an impulse. A subscript is added to designate specific tracers. Thus, $h_D(t)$ denotes the "permeating" or "diffusible" tracer; $h_E(t)$ signifies the extracellular tracer; and $h_R(t)$ is used to represent the intravascular "reference" tracer.

16-7.2. Substrate metabolism by sequential reactions.

The impetus for the development of this model was the need to analyze data from a series of experiments aimed at understanding the utilization of adenosine in the myocardium. These experiments used radio-labeled adenosine at tracer concentration (i.e., a concentration low enough that it could be assumed that the pre-existing concentration of unlabeled adenosine was not changed by the addition of the labeled adenosine) and the data were collected over a period of 1-2 minutes. This led to a design that featured a linear sequence of nonreversible reactions.

A set of six substrates in a linear reaction chain are modeled in MSID4, but this may be extended arbitrarily. The sequence can be diagrammed as:

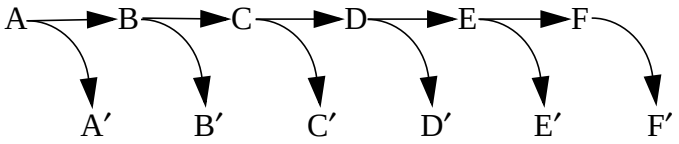

Diagram 16-1

The primed letters represent tracer trapped in some form but not reacted as a part of the sequence. In the description of the four-region BTEX model given above, the consumption term accounts for all processes that cause clearance of the tracer from the region (e.g., sequestration and chemical transformation). In the MSID4 model however, these processes are separated rather than being lumped together. Focusing on a single reaction in the diagram above, the process can be represented as:

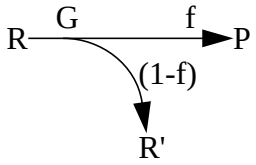

Diagram 16-2

The total clearance of reactant (*R*) during each time step of the solution is governed by the first-order rate constant *G*. Of the total amount cleared, some fraction, *f*, is transformed into the product (*P*). This product appears in the regions of its own BTEX model where the reaction occurred; it can diffuse across membranes and may undergo further reactions. The remainder of the reactant cleared during the time step is transformed into a sequestered form of the reactant (*R′*)

that neither undergoes further chemical transformation nor diffuses across barriers. This reaction sequence modifies Eq. 16-10 through Eq. 16-13 by adding an additional term that accounts for the input from chemical transformation. A general equation for the concentration of a product in any region is

$$\frac{\partial_{\mathrm{P}} C_{\mathrm{r}}}{\partial t} = -\,{}_{\mathrm{P}}X_{\mathrm{r}} + {}_{\mathrm{P}}D_{\mathrm{r}}\frac{\partial_{\mathrm{P}}^{2} C_{\mathrm{r}}}{\partial x^{2}} - \frac{{}_{\mathrm{P}}G_{\mathrm{r}}}{{}_{\mathrm{P}}V'_{\mathrm{r}}}\,{}_{\mathrm{P}}C_{\mathrm{r}} + {}_{\mathrm{P}}f_{\mathrm{r}}\,\frac{{}_{\mathrm{R}}G_{\mathrm{r}}}{{}_{\mathrm{P}}V'_{\mathrm{r}}}\,{}_{\mathrm{R}}C_{\mathrm{r}}, \tag{16-14}$$

where the leading subscript specifies either the reactant or product, and the trailing subscript, *r*, specifies the region. The first term on the right in Eq. 16-14, ${}_{\mathrm{P}}X_{\mathrm{r}}$, is the summation of all permeation terms for the product in that region and, in the case of the plasma region, the convection term as well. The second and third terms are the axial diffusion and consumption terms respectively from those equations. The last term is the input from chemical transformation of the reactant that produces this substrate as its product. Thus the production is the consumption of the preceding reactant substrate in the reaction sequence. Since substrate *A* is not a reaction product, ${}_{\mathrm{R}}G_{\mathrm{r}}$ is equal to zero for substrate A.

Using the same nomenclature as in Eq. 16-14, the equation for the sequestered form of the reactant is

$$\frac{\partial_{\mathrm{R}'} C_{\mathrm{r}}}{\partial t} = {}_{\mathrm{R}'}D_{\mathrm{r}}\frac{\partial_{\mathrm{R}'}^{2} C_{\mathrm{r}}}{\partial x^{2}} + (1 - {}_{\mathrm{R}}f_{\mathrm{r}})\frac{{}_{\mathrm{R}}G_{\mathrm{r}}}{{}_{\mathrm{R}'}V'_{\mathrm{r}}}\,{}_{\mathrm{R}}C_{\mathrm{r}}\,. \tag{16-15}$$

The first term accounts for axial diffusion within the region and the second is the production term. The latter is the same as in Eq. 16-14 except that the multiplier is $(1 - {}_{\mathrm{R}}f_{\mathrm{r}})$, thus assuring mass balance. For substrate *F*, ${}_{\mathrm{R}}f_{\mathrm{r}}$ is equal to zero; thus, all cleared tracer is sequestered. The transmembrane diffusion term is absent since the sequestered tracer does not cross barriers. Eq. 16-15 must, however, be modified in the case of the plasma region. Even though tracer in the sequestered form does not cross the capillary barriers, it is carried down the capillary and into the outflow by convection. Thus, for the plasma the equation is

$$\frac{\partial_{\mathrm{R}'} C_{\mathrm{p}}}{\partial t} = -\frac{F_{\mathrm{p}} L}{{}_{\mathrm{R}'}V_{\mathrm{p}}}\cdot\frac{\partial_{\mathrm{R}'} C_{\mathrm{p}}}{\partial x} + {}_{\mathrm{R}'}D_{\mathrm{p}}\frac{\partial_{\mathrm{R}'}^{2} C_{\mathrm{p}}}{\partial x^{2}} + (1 - {}_{\mathrm{R}}f_{\mathrm{p}})\frac{{}_{\mathrm{R}}G_{\mathrm{p}}}{{}_{\mathrm{R}'}V'_{\mathrm{p}}}{}_{\mathrm{R}}C_{\mathrm{p}}\,. \tag{16-16}$$

Several assumptions are implicit in this formulation of the model and we now state them explicitly. All reactions are unidirectional, and the reaction rates are all first order. The reaction rates are not subject to control by the concentration of the reactant or product or by any other mechanism. The reactions form a linear sequence without feedback and the pool size for the sequestered form of the substrates is infinite (i.e., there is no return flux). We will come back to some of these limitations in the Discussion.

16-7.3. Basic modeling analysis of the MID experimental data set

The modeling analysis can proceed immediately when an input function has been defined. When deconvolution is needed to produce the input function, then the intravascular transport must first be defined, as in the next section. If the input is known, or if it is approximated by an arbitrary

input waveform such as a lagged-normal density curve (Bassingthwaighte, 1966) or a gamma variate function (Thompson et al., 1964), then we proceed directly to the modeling of intravascular transport.

16-7.4. Intravascular transport

As shown in Fig. 16-4, there are three components of the blood of the organ. The first is a common large vessel representing large arteries and veins and leading to a set of parallel paths. Each of up to 20 parallel paths consists of an operator representing vascular transport through medium size vessels without exchange (component two) and the blood–tissue exchange operator (component three). The total blood volume of the heart is about 0.15 ml/g; of this the common path volume, V_{LV}, is about 0.03 ml/g, the medium vessels, V_{MV}, 0.07 ml/g and the capillaries, V_p, about 0.05 ml/g depending on driving pressures, flows, and state of vasodilation.

To account for both the dispersion and delay due to transport through medium size non-exchanging arteries and veins, an operator is included in series with each capillary tissue unit. The "medium vessel operator" is composed of a pure delay line in series with a dispersive operator, a fourth-order differential operator made up of two second-order operators in series. The parameters of the fourth-order operator are those given by Bassingthwaighte, Knopp and Anderson (1970) which result in its relative dispersion (coefficient of variation of the impulse response) being 48%. By setting the delay operator to provide 60% of the total mean transit time of the medium vessel operator, the relative dispersion of the medium vessel operator is set at 0.48 (1.0-0.6) or 19.2% (King et al., 1993). This is approximately the level of dispersion found for arteries by Bassingthwaighte (1966). The operator accounts for both arterial and venous dispersion (convolution being commutative), and if venous dispersion is relatively greater than arterial the total dispersion may be a bit smaller than is realistic. The same fractional volume was assumed for high and low flow regions, V_{MV} = 0.07 ml/g; the transit times were inversely proportional to the flows in the individual pathways. This medium vessel operator has the advantage of accounting for both intravascular dispersion and for regional variation in transit times. By being dispersive it offers an improvement over the pure delay lines used by Rose and Goresky (1976) while simultaneously accounting for the association between medium vessel and capillary transit times that they advocate.

Transport within capillaries is dispersive (Crone et al., 1978). The Lagrangian numerical method matching time and space steps (Bassingthwaighte, 1974; Bassingthwaighte, Wang and Chan, 1989) is non-dispersive, but the dispersion process is applied at each time step using a classical diffusion expression (Bassingthwaighte, Chan and Wang, 1992) where D represents the dispersion due to all operative processes: molecular diffusion, eddy currents at branches, velocity profiles and disturbed flow.

16-7.5. Finding the input function when it was not measured

When the input function is not measured, then the model input at the point where the parallel pathways diverge, that is, the exit from the large vessel operator, is determined either by deconvolution from the observed $h_R(t)$ or by optimizing the form of an assumed input function until the observed output vascular $h_R(t)$ is matched by the model solution. An example is shown in Fig. 16-6. The approach is to estimate the form of the intravascular transport from inflow to outflow, through the set of parallel paths, then to deconvolute by a smoothing, stabilized method to get the input function. The result is then checked by convolution of the input with the intravascular transport function. That the model solution using the input curve obtained by

deconvolution should fit the actual $h_R(t)$ should evoke no surprise since that simply amounts to reconvolution. The deconvolution process itself is complex. We use a variation of the method of Bronikowski et al. (1980) that constrains the technique to producing wave forms without negative or highly oscillatory components. The use of numerical deconvolution (Maseri et al., 1970) is not usually workable because the result is ordinarily a highly oscillatory function. Deconvolution is a kind of a differentiation process, and is generally unreliable unless considerable care is taken. Often it is better to guess the input function than to deconvolute. The safest guess is to assume a narrow pulse input, and then account for the dispersion between the inflow and the outflow as intravascular dispersion. Since it is assumed that all the tracers undergo the same intravascular dispersion this introduces no error into the estimation of the values of the parameters for the tracer exchange processes when we are dealing with tracer dilution by a linear stationary system.

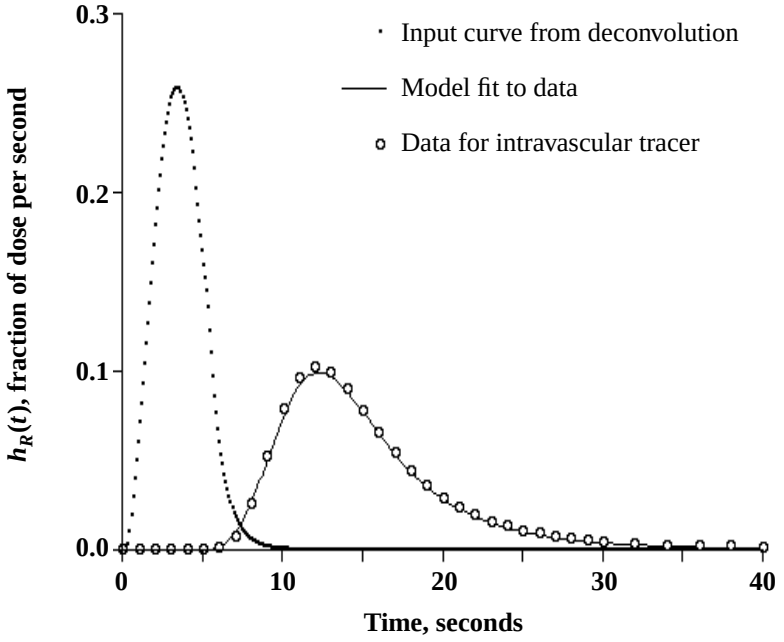

Figure 16-6: Deconvolution from the curve of reference data produces a smooth unimodal input. Capillary and small vessel volumes are assumed from anatomic data and the observed mean transit time volume, $F \cdot t_R$. Reconvolution, giving a good fit, is merely a test of the numerical methods and does not guarantee that C_{in} is correct.

16-7.6. The extracellular reference indicator

The diffusion of the extracellular reference tracer through the clefts between the endothelial cells is the event by which this tracer becomes separated from the intravascular reference tracer. The extracellular tracer transport function is labelled $h_E(t)$. While its area must be identical to that of the intravascular reference tracer, the form of its outflow curve is not: it is lower-peaked than the intravascular marker, because of the partial and transient loss from the intravascular region. The tracer that escapes through these clefts is diluted in the volume of the interstitial fluid. Its return from the ISF is again retarded by the process of diffusion from the ISF through the clefts back into the capillary space. Its mean transit time is necessarily longer, and by conservation, can be exactly stated:

$$\bar{t}_E = (V_{cap} + V_{isf}) / F_p$$

There is a usually unstated assumption built into our thinking with respect to the permeating tracers. It is that the exchange is occurring solely between the blood in the capillary and the surrounding region. In fact, it has been recognized repeatedly that the small venules are also permeable to small molecules; this means in reality that while we estimate "capillary permeability", this is really a composite of capillary and small venular permeability. The next assumption ordinarily glossed over is that the intravascular indicator does not escape from the vascular space. This is really a pretty good assumption for most such experiments and can be checked by mass balance. The sum of the tracer concentrations times the volumes of exchange outflow sample should equal the dose of each of the tracers injected. For both the intravascular and the extracellular tracer, this check should be done on every dilution curve as a matter of routine. Acceptable accuracy is within ± 2% of the injected dose. While single-pass extraction of albumin is normally a small fraction of a percent, permeation does actually occur and plasma and ISF albumin concentrations equilibrate after many minutes.

16-7.7. The permeant or reactant substrate

Data on the permeant solute is normalized in exactly the same way, but in this case the total dose may not be recovered in the outflow if there is retention within the organ and the collection period is not extended for a very long time. Of course if there is a metabolic transformation within the organ and total retention of the product of the reaction, then it will never emerge. The fractional recovery then may give some clue as to the fate of the permeating solute. In experiments where external detection of a gamma-emitting permeant is feasible, then the total dose is equivalent to the sum of the accumulated outflow fractional doses plus what is retained within the organ:

$$\text{Total dose} = \int_0^T h_D(t)dt + R(T),$$

at any time T during the outflow. When beta-emitting tracers are being used, one can estimate $R(t)$ by taking the whole of the tissue at the time of the last outflow sample, i.e., at time t, freezing and grinding it up to find the value for $R(t)$. When there is transformation occurring within the tissue one will normally want to refine this idea by separating the various forms of the reaction products to obtain values for the retention of the individual reaction products. These individual values then become a part of the data set for model analysis, and allow a more refined estimation of the rates of the various reactions.

16-8. Constraints on parameter ranges

16-8.1. Mass conservation

Finding the dose calibration and the fractional recoveries of each of the tracers is the first step in making sure of mass conservation. The second is that for the permeant solute which participates in reaction sequences, the sum of the unreacted solute and the amounts of all the reaction products in the outflow samples and in the tissue should add up to the dose injected, neither more nor less. While this is simply stated, in practice it requires deliberate care to achieve, and when there are several, chemically separated reaction products it is difficult to achieve 5% accuracy.

Another aspect of mass balance is in the modeling itself. The model solutions should provide mass balance within a small fraction of 1% when one performs the summations analogous to what one does for the experimental data. A mass balance check, for example, is the flow times the integral of the concentrations in the inflow, and the same for the outflow. Both should be checked. If the integrals are not identical and if there is no "material" remaining in the model operator itself in one form or another, then there is a computational error and the model is invalid. Since an accumulation of numerical errors can give a result summing up to either too much or too little material, this is an essential check on the model implementation.

16-8.2. Anatomical and physiological data

Volumes of distribution should add up appropriately. The sum of the fractional water contents of the several components of the tissue should add up exactly to the total water content of the tissue, as measured by weighing the tissue when wet, drying it at 50 to 60C for 48 hours and reweighing. This calculation should take into account the expected water fractions of red blood cells, plasma, the volumes of non-exchanging vessels, of capillaries, of the ISF and the cells. RBC are the driest cells of the body, about 65% water; plasma is 94% water, and cells and ISF are more variable. The heart water content, if it is not edematous, is remarkably uniform, about 0.78 ml/g water with a standard deviation of about 0.01 ml/g. With edema, usually mainly expansion of the interstitial space, the water fraction rises to a maximum of about 0.84 ml/g, above which the heart ceases to beat. This is actually a formidable dilution of the solid content, from 0.22 ml/g down to 0.16 ml/g so there is little wonder that isolated perfused hearts simply stop functioning when they get this soggy. Other constraints come from data on the volumes of capillaries and on the total blood volume of the organ. With capillarity of 3000 capillaries per mm^2 cross section and average diameters of 5 microns, the capillary volume is about 0.055 ml/g (using tissue density of 1.063 g/ml) (Yipintsoi et al., 1972). An important factor in this approach is that the assumption of a value such as $V_p = 0.055$ ml/g is not critical to the subsequent analysis: Wangler et al. (1989), in their Fig. 4, showed that large error in choosing fixed values of V_p had little influence on estimates of the transport parameters. Since the total blood volume in a heart is about 0.12 to 0.15 ml/g at normal flows but higher when flows are raised in specific situations, e.g., in the presence of hyperosmolar, vasodilating contrast agents (Koiwa et al., 1986), this estimate provides also a constraint to limit the range of the sum of the volumes of the arteries and the veins. More comprehensive sets of data on individual organs and species need to be acquired. An attempt by Vinnakota and Bassingthwaighte (2004) to assemble data on the composition of myocardium met with success only for the rat heart, other species lacking so much information that a complete mass and composition balance would be only achievable with an uncomfortably large number of assumptions. See Chapter 9 for the matrix approach to finding a self consistent description of tissue composition.

Likewise, data from stereological studies on tissue composition can provide constraints. The different cell types and the different fractions of nuclear and mitochondrial content of the different cell types can provide additional useful values. So far here we have discussed constraints on estimates of volumes, therefore on the volumes of distribution that can be used in the modeling analysis. If an estimate of a volume of distribution for a solute appears via modeling analysis to be significantly larger than the anatomical volume, then one must ask if this can be explained by intracellular binding or some other physiological process. Sometimes it is difficult to distinguish retention in the tissue by the intracellular binding of a substrate from the long-term retention of its

reaction product. On such occasions one must contemplate undertaking the relevant chemical analysis of tissue samples.

16-9. Summary

The general theory of input-output relationships is applicable to the study of any system where one has access to signals at the input and can observe the resultant responses at the output. The general theory is derived for linear stationary systems, that is, those with time-invariant responses to a given input, and with responses proportional to the input. While in modern indicator dilution studies we deal with nonlinear systems, that is best done using specific models to serve as analogs of the system; even in these cases we depend upon certain aspects of the system to be linear and stationary; in particular, the responses to an intravascular reference tracer and to an extracellular reference marker should fall under the standard theory. This theory therefore provides a basis for the linear and nonlinear studies which follow.

16-10. Problems

1. In MID studies one wishes to analyze a sequence of outflow samples using HPLC to separate metabolites. Since reactions continue to occur in the blood after the samples are collected, it is important to mix the sampled blood with a “stopping solution” to stop reactions which would compromise the interpretation of the data. What the classes of chemicals you would explore using for a specific MID study? Relate the specific experiment to the agents you would choose. How would you determine the efficacy of your chosen agents?
2. The reference tracers defining the transport functions of the intravascular space and the extracellular fluid space are assumed to be 100% conserved. How do you test, experimentally, to assure yourself that this is the case? What are the sources of error in doing this check, which is a control for mass balance?
3. List and comment on the use of different sites of tracer injection when doing MID studies of the kidney in an intact animal or human to obtain estimates of transmembrane kinetic parameters. Include venous versus arterial sites, and different arterial sites. Consider frequency content of the input versus that of the impulse response function of the kidney for the different tracers.
4. Write a set of PDEs for an MID experiment for tracers in a situation where there is steady state with respect to the concentrations of the tracees. The equations should include those for an intravascular tracer, an extracellular tracer, and for a tracer that enters cells and is metabolized there to form a product. Include the equations for the product, assuming that it too can permeate the cell membrane and be washed out.
5. “Tracer experiments permit linear systems analysis.” Write the equations which justify this statement.
6. In determining the exchange and reaction parameters for a substrate in a particular organ it is useful to determine the probability density function of regional flows and to take this into account in the modeling analysis of the MID data. Describe how the pdf of regional flows is used? What resolution in the pdf would you use in translating it into a finite number of parallel pathways? Discuss trade-offs in your choice. What are the directions of the errors in parameter estimation when heterogeneity of regional flows is ignored?

7. How would you measure the heterogeneity of regional flows in a cell culture system where the cells are growing on glass or latex beads? What form would you expect for an extracellular tracer that does not bind to cell surface receptors or non-specific binding sites? What would be the influence of such receptors or binding sites on the outflow curve for this extracellular reference marker? How would external binding affect your use of this substance as a reference tracer in the modeling analysis of a substance which enters the cells.
8. "Ideally, reference tracers, whether intravascular or extravascular, might be most directly useful if they are flow-limited in their transport." Define flow-limited exchange. Discuss the pros and cons of the quoted statement. Consider the liver versus the heart versus the brain when discussing the extracellular reference tracer usage.
9. Intravascular transport functions for individual organs are usually unimodal. Describe situations in which they might be bimodal or multimodal? Will whole body transport functions, from aorta to vena cava be unimodal, and if not, what are your expectations about the sources of deviations from unimodality?
10. This chapter has focused on the MID technique, using multitracer outflow concentration-time curves from a single organ. How would you translate the major ideas so that you could analyze data from external detection techniques like PET and MRI to obtain estimates of regional flows and transport and reaction parameters?
11. Compare and contrast MID and PET studies to obtain information capillary permeability to an extracellular marker such as sucrose. Consider the tracers, the data acquisition and the analysis.

16-11. References

Bassingthwaighte JB, Ackerman FH, and Wood EH. Applications of the lagged normal density curve as a model for arterial dilution curves. *Circ Res* 18: 398-415, 1966.

Bassingthwaighte JB. Plasma indicator dispersion in arteries of the human leg. *Circ Res* 19: 332-346, 1966.

Bassingthwaighte JB. Blood flow and diffusion through mammalian organs. *Science* 167: 1347-1353, 1970.

Bassingthwaighte JB, Knopp TJ, and Anderson DU. Flow estimation by indicator dilution (bolus injection): Reduction of errors due to time-averaged sampling during unsteady flow. *Circ Res* 27: 277-291, 1970.

Bassingthwaighte JB, Dobbs WA, and Yipintsoi T. Heterogeneity of myocardial blood flow. In: *Myocardial Blood Flow in Man: Methods and significance in coronary disease,* edited by Maseri A. Torino, Italy: Minerva Medica, 1972, p. 197-205.

Bassingthwaighte JB. The measurement of blood flows and volumes by indicator dilution. In: *Medical Engineering,* edited by Ray CD. Chicago: Yearbook Publishers, 1974, p. 246-260.

Bassingthwaighte JB, Yipintsoi T, and Harvey RB. Microvasculature of the dog left ventricular myocardium. *Microvasc Res* 7: 229-249, 1974.

Bassingthwaighte JB. A concurrent flow model for extraction during transcapillary passage. *Circ Res* 35: 483-503, 1974.

Bassingthwaighte JB and Goresky CA. Modeling in the analysis of solute and water exchange in the microvasculature. In: *Handbook of Physiology. Sect. 2, The Cardiovascular System. Vol IV, The Microcirculation,* edited by Renkin EM and Michel CC. Bethesda, MD: Am. Physiol. Soc., 1984, p. 549-626.

Bassingthwaighte JB, Chinard FP, Crone C, Goresky CA, Lassen NA, Reneman RS, and Zierler KL. Terminology for mass transport and exchange. *Am J Physiol Heart Circ Physiol* 250: H539-H545, 1986.

Bassingthwaighte JB, King RB, and Roger SA. Fractal nature of regional myocardial blood flow heterogeneity. *Circ Res* 65: 578-590, 1989.

Bassingthwaighte JB, Wang CY, and Chan IS. Blood-tissue exchange via transport and transformation by endothelial cells. *Circ Res* 65: 997-1020, 1989.

Bassingthwaighte JB, Malone MA, Moffett TC, King RB, Chan IS, Link JM, and Krohn KA. Molecular and particulate depositions for regional myocardial flows in sheep. *Circ Res* 66: 1328-1344, 1990.

Bassingthwaighte JB, Chan IS, and Wang CY. Computationally efficient algorithms for capillary convection-permeation-diffusion models for blood-tissue exchange. *Ann Biomed Eng* 20: 687-725, 1992.

Bassingthwaighte JB and Beard DA. Fractal ^{15}O-water washout from the heart. *Circ Res* 77: 1212-1221, 1995.

Bohr C. U*:ber die spezifische Ta*:tigkeit der Lungen bei der respiratorischen Gasaufnahme und ihr Verhalten zu der durch die Alveolarwand stattfindenden Gasdiffusion. *Skand Arch Physiol* 22: 221-280, 1909.

Bridge JHB, Bersohn MM, Gonzalez F, and Bassingthwaighte JB. Synthesis and use of radiocobaltic EDTA as an extracellular marker in rabbit heart. *Am J Physiol Heart Circ Physiol* 242: H671-H676, 1982.

Bronikowski TA, Linehan JH, and Dawson CA. A mathematical analysis of the influence of perfusion heterogeneity on indicator extraction. *Math Biosci* 52: 27-51, 1980.

Buckberg GD, Luck JC, Payne BD, Hoffman JIE, Archie JP, and Fixler DE. Some sources of error in measuring regional blood flow with radioactive microspheres. *J Appl Physiol* 31: 598-604, 1971.

Bukowski T, Moffett TC, Revkin JH, Ploger JD, and Bassingthwaighte JB. Triple-label β liquid scintillation counting. *Anal Biochem* 204: 171-180, 1992.

Chinard FP, Vosburgh GJ, and Enns T. Transcapillary exchange of water and of other substances in certain organs of the dog. *Am J Physiol* 183: 221-234, 1955.

Crone C. The permeability of capillaries in various organs as determined by the use of the 'indicator diffusion' method. *Acta Physiol Scand* 58: 292-305, 1963.

Crone C, Frøkjaer-Jensen J, Friedman JJ, and Christensen O. The permeability of single capillaries to potassium ions. *J Gen Physiol* 71: 195-220, 1978.

Deussen A and Bassingthwaighte JB. Modeling [^{15}O]oxygen tracer data for estimating oxygen consumption. *Am J Physiol Heart Circ Physiol* 270: H1115-H1130, 1996.

Dible JH. Is fatty degeneration of the heart muscle a phanerosis?. *J Pathol Bacteriol* 39: 197-207, 1934.

Diem K. *Documenta Geigy. Scientific Tables.* Ardsley, N. Y.: Geigy Pharmaceuticals, 1962.

Fox, IJ, WF Sutterer, and EH Wood. TITLE?? J. Appl. Physiol. 11: 390- ??, 1957.

Glenny R, Robertson HT, Yamashiro S, and Bassingthwaighte JB. Applications of fractal analysis to physiology. *J Appl Physiol* 70: 2351-2367, 1991.

Gonzalez F and Bassingthwaighte JB. Heterogeneities in regional volumes of distribution and flows in the rabbit heart. *Am J Physiol Heart Circ Physiol* 258: H1012-H1024, 1990.

Gonzalez-Fernandez JM. Theory of the measurement of the dispersion of an indicator in indicator-dilution studies. *Circ Res* 10: 409-428, 1962.

Goresky CA. A linear method for determining liver sinusoidal and extravascular volumes. *Am J Physiol* 204: 626-640, 1963.

Goresky CA, Ziegler WH, and Bach GG. Capillary exchange modeling: Barrier-limited and flow-limited distribution. *Circ Res* 27: 739-764, 1970.

Gorman MW, Bassingthwaighte JB, Olsson RA, and Sparks HV. Endothelial cell uptake of adenosine in canine skeletal muscle. *Am J Physiol Heart Circ Physiol* 250: H482-H489, 1986.

Grant PE and Lumsden CJ. Fractal analysis of renal cortical perfusion. *Invest Radiol* 29: 16-23, 1994.

Hamilton WF, Moore JW, Kinsman JM, and Spurling RG. Studies on the circulation. IV. Further analysis of the injection method, and of changes in hemodynamics under physiological and pathological conditions. *Am J Physiol* 99: 534-551, 1932.

Harris TR, Bernard GR, Brigham KL, Higgins SB, Rinaldo JE, Borovetz HS, Sibbald WJ, Kariman K, and Sprung CL. Lung microvascular transport properties measured by multiple indicator dilution methods in patients with adult respiratory distress syndrome. A comparison between patients reversing respiratory failure and those failing to reverse. *Am Rev Respir Dis* 141: 272-280, 1990.

King RB, Bassingthwaighte JB, Hales JRS, and Rowell LB. Stability of heterogeneity of myocardial blood flow in normal awake baboons. *Circ Res* 57: 285-295, 1985.

King RB, Deussen A, Raymond GR, and Bassingthwaighte JB. A vascular transport operator. *Am J Physiol Heart Circ Physiol* 265: H2196-H2208, 1993.

King RB, Raymond GM, and Bassingthwaighte JB. Modeling blood flow heterogeneity. *Ann Biomed Eng* 24: 352-372, 1996.

King RB. Modeling membrane transport. *Advances in Food and Nutrition Research* 40: 243-262, 1996.

Koiwa Y, Bahn RC, and Ritman EL. Regional myocardial volume perfused by the coronary artery branch: estimation *in vivo*. *Circulation* 74: 157-163, 1986.

Kuikka J, Levin M, and Bassingthwaighte JB. Multiple tracer dilution estimates of D- and 2-deoxy-D-glucose uptake by the heart. *Am J Physiol Heart Circ Physiol* 250: H29-H42, 1986.

Lassen NA and Perl W. *Tracer Kinetic Methods in Medical Physiology.* New York: Raven Press, 1979.

Lumsden CJ and Silverman M. Exchange of multiple indicators across renal-like epithelia: a modeling study of six physiological regimes. *Am J Physiol* 251 (Renal. Fluid. Elect. Physiol. 20): F1073-F1089, 1986.

Malcorps CM, Dawson CA, Linehan JH, Bronikowski TA, Rickaby DA, Herman AG, and Will JA. Lung serotonin uptake kinetics from indicator-dilution and constant-infusion methods. *J Appl Physiol* 57 (*Respirat. Environ. Exercise Physiol.*): 720-730, 1984.

Maseri AP, Caldini S, Permutt S, and Zierler KL. Frequency function of transit times through dog pulmonary circulation. *Circ Res* 26: 527-543, 1970.

Meier P and Zierler KL. On the theory of the indicator-dilution method for measurement of blood flow and volume. *J Appl Physiol* 6: 731-744, 1954.

Polimeni PI. Extracellular space and ionic distribution in rat ventricle. *Am J Physiol* 227: 676-683, 1974.

Renkin EM. Transport of potassium-42 from blood to tissue in isolated mammalian skeletal muscles. *Am J Physiol* 197: 1205-1210, 1959.

Renkin EM. Exchangeability of tissue potassium in skeletal muscle. *Am J Physiol* 197: 1211-1215, 1959.

Rickaby DA, Linehan JH, Bronikowski TA, and Dawson CA. Kinetics of serotonin uptake in the dog lung. *J Appl Physiol* 51 (*Respirat. Environ. Exercise Physiol.* 2): 405-414, 1981.

Rose CP and Goresky CA. Vasomotor control of capillary transit time heterogeneity in the canine coronary circulation. *Circ Res* 39: 541-554, 1976.

Rose CP, Goresky CA, and Bach GG. The capillary and sarcolemmal barriers in the heart: An exploration of labeled water permeability. *Circ Res* 41: 515-533, 1977.

Sangren WC and Sheppard CW. A mathematical derivation of the exchange of a labeled substance between a liquid flowing in a vessel and an external compartment. *Bull Math Biophys* 15: 387-394, 1953.

Sapirstein LA. Regional blood flow by fractional distribution of indicators. *Am J Physiol* 193: 161-168, 1958.

Sokoloff L, Reivich M, Kennedy C, Des Rosiers MH, Patlak CS, Pettigrew KD, Sakurada O, and Shinohara M. The [^{14}C]deoxyglucose method for the measurement of local cerebral glucose utilization: Theory, procedure, and normal values in the conscious and anesthetized albino rat. *J Neurochem* 28: 897-916, 1977.

Thompson HK, Starmer CF, Whalen RE, and McIntosh HD. Indicator transit time considered as a gamma variate. *Circ Res* 14: 502-515, 1964.

Vinnakota and Bassingthwaighte Am J Physiol Heart Circ Physiol 2004

Wangler RD, Gorman MW, Wang CY, DeWitt DF, Chan IS, Bassingthwaighte JB, and Sparks HV. Transcapillary adenosine transport and interstitial adenosine concentration in guinea pig hearts. *Am J Physiol Heart Circ Physiol* 257: H89-H106, 1989.

Yipintsoi T, Tancredi R, Richmond D, and Bassingthwaighte JB. Myocardial extractions of sucrose, glucose, and potassium. In: *Capillary Permeability (Alfred Benzon Symp. II),* edited by Crone C and Lassen NA. Copenhagen: Munksgaard, 1970, p. 153-156.

Yipintsoi T, Scanlon PD, and Bassingthwaighte JB. Density and water content of dog ventricular myocardium. *Proc Soc Exp Biol Med* 141: 1032-1035, 1972.

Yipintsoi T, Dobbs WA Jr., Scanlon PD, Knopp TJ, and Bassingthwaighte JB. Regional distribution of diffusible tracers and carbonized microspheres in the left ventricle of isolated dog hearts. *Circ Res* 33: 573-587, 1973.

Zierler KL. Theoretical basis of indicator-dilution methods for measuring flow and volume. *Circ Res* 10: 393-407, 1962.

Zierler KL. Equations for measuring blood flow by external monitoring of radioisotopes. *Circ Res* 16: 309-321, 1965.